Wind and Structures, Vol. 5, No. 2~4 (2002) 101-114
DOI: http://dx.doi.org/10.12989/was.2002.5.2_4.101

A comparative study of numerical methods for fluid structure interaction analysis in long-span bridge design

Guido Morgenthal† and Allan McRobie‡

Department of Engineering, University of Cambridge, Trumpington Street, Cambridge CB2 1PZ, U.K.

Abstract. Both a Finite Volume and a Discrete Vortex technique to solve the unsteady Navier-Stokes equations have been employed to study the air flow around long-span bridge decks. The implementation and calibration of both methods is described alongside a quasi-3D extension added to the DVM solver. Applications to the wind engineering of bridge decks include flow simulations at different angles of attack, calculation of aerodynamic derivatives and fluid-structure interaction analyses. These are being presented and their specific features described. If a numerical method shall be employed in a practical design environment, it is judged not only by its accuracy but also by factors like versatility, computational cost and ease of use. Conclusions are drawn from the analyses to address the question of whether computer simulations can be practical design tools for the wind engineering of bridge decks.

Key words: computational bridge aerodynamics; Discrete Vortex Method; Finite Volume Method; vortex shedding.

1. Introduction

Various fluid-structure interaction phenomena have to be considered in long-span bridge design, e.g., vortex induced oscillations and flutter. Earlier work on the topic of numerical simulations has been conducted by one of the authors investigating the feasibility of a fully-coupled Finite Element approach (Frandsen and McRobie 1999), which yielded promising results in predicting aeroelastic response phenomena.

Herein, work on two further numerical methods, the Discrete Vortex Method (DVM) and the Finite Volume Method (FVM), is described. The merits and problems of both shall be discussed in detail and conclusions regarding their applicability to the wind engineering of bridge decks will be drawn.

2. The Discrete Vortex Method

The authors have developed a computer code for numerical solution of the unsteady incompressible Navier-Stokes equations by a Lagrangian vortex formulation. The Discrete Vortex Method has attracted great interest in recent years, mainly concerned with applications in bluff body aerodynamics, e.g., in

† EPSRC Research Student
‡ Lecturer

bridge engineering by Larsen and Walther (1998).

The Discrete Vortex Method is derived from the knowledge that in a high-Reynolds number flow there are three distinct regions: the viscous, rotational boundary layer, the wake and an inviscid outer region, which is usually irrotational. The idea is to introduce the vorticity at a certain region or point and then to trace it through the flow by using the vorticity equation derived from the Navier-Stokes equation, as outlined in Leonard (1980). Herein we assume that the fluid is incompressible, two-dimensional, single-phase, homogeneous and that temperature variation has a negligible impact on the flow field. The main difference to other methods is that the DVM is grid-free and thus data input is much facilitated. The computational effort can, however, be large since all mutual vortex interactions have to be considered at each time step, thus (for the simplest schemes) making the cost proportional to the square of the number of vortices in the domain.

The code described here makes use of an inviscid formulation, employing a simple Euler scheme for the convection process. At each time step all surface vorticity is released as discrete Rankine vortices introduced at fixed points approximately half a panel length away from the surface. A cell-to-cell algorithm as proposed by Leonard (1980) was implemented, resulting in considerable reductions in computation time.

It is important to note that the numerical solution procedure involves a number of parameters that strongly influence the quality of the solution, namely the level of noise in the signals obtained for the pressures and the body forces. These are mainly

- the non-dimensional time step $t^* = tU / l$ (where l is any reference length, here the panel length),
- distance of release points from surface,
- vortex core radius.

Even though time averaging improves the force signals, care needs to be exercised in order for the physical processes still to be represented in the solution. Experience is necessary to find a set of parameters that yield a robust solution and good results. While a wake is usually formed without problems, the formation region, i.e., the boundary layer, is of great importance and its structure can indicate whether a stable solution is achieved. The calibration procedure found to be most favourable was to perform a Fast Fourier Transform on the signals and to adjust the numerical parameters until a clear solution is obtained. Pre-calibration of the DVM for ready-use in a design office is difficult to achieve and experience from the user will always be required. The analyses presented herein were performed with core radii of the order of half a panel length. Non-dimensional time steps were between 0.5 and 1.

2.1. Analyses on static bodies

A number of validation tests were carried out using the DVM code developed. Vortex shedding analyses on static circular cylinders are reported in Morgenthal (2000). Another standard case for aerodynamic simulations, more closely related to bridge deck analysis, are rectangular cylinders. Their vortex shedding response is different from that of circular cylinders in that the separation points are fixed at the sharp corners. However, reattachment may occur on long faces and it is crucial for numerical models to be capable of capturing this. Deniz and Staubli (1998) compiled results from a number of vortex shedding simulations from rectangular cylinders of various aspect ratios and this was used to validate the DVM code. Fig. 1 shows non-dimensional shedding frequency plotted against the aspect ratio.

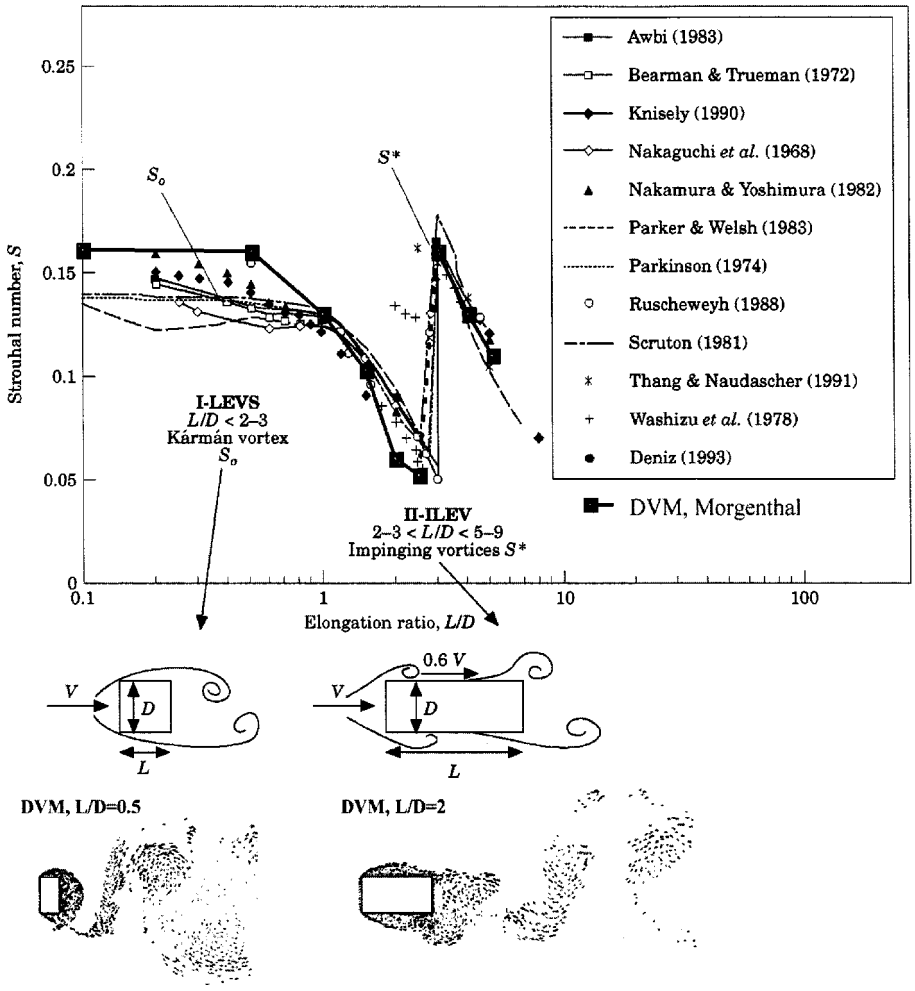

Fig. 1 Vortex shedding from rectangular cylinders, Strouhal number $St(D)$ dependence on aspect ratio, after Deniz and Staubli (1998) with added results from DVM simulations

The deck of the Storebœlt suspension bridge was chosen for calibration analyses because its aerodynamic properties have been extensively studied and are well documented in the literature. DVM calculations of the static deck were performed at first. Fig. 2 shows an averaged pressure distribution obtained from wind tunnel tests at the Danish Maritime Institute (DMI) 1993 and the pressure distribution predicted by the DVM. Even though the bridge deck aerodynamics are much more complex than the cylinder test cases due to flow reattachment and a complex wake formation region, the pressure distribution is remarkably well captured. A sample picture of the vorticity distribution is shown in Fig. 3.

A Fourier spectrum of the lift force signal is given in Fig. 4 for a free stream velocity of 8 m/s. The Strouhal number $St(D)$ was evaluated to 0.19.

The results for the main aerodynamic properties are given in Table 1 alongside values from other investigations. Both force coefficients and the shedding frequency compare well.

The DVM was also applied to this cross section to perform calculations at different angles of

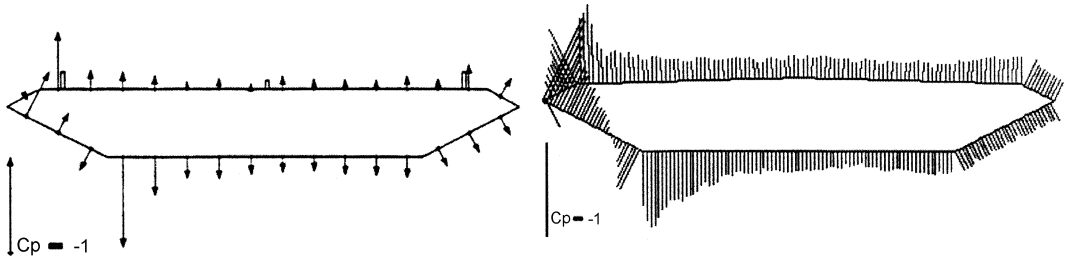

Fig. 2 Storeboelt Bridge, normalised pressure distribution obtained from wind tunnel tests (DMI and SINTEF 1993) and with DVM (Morgenthal)

Fig. 3 Vortex shedding from static Storeboelt Bridge, instantaneous vorticity field from DVM

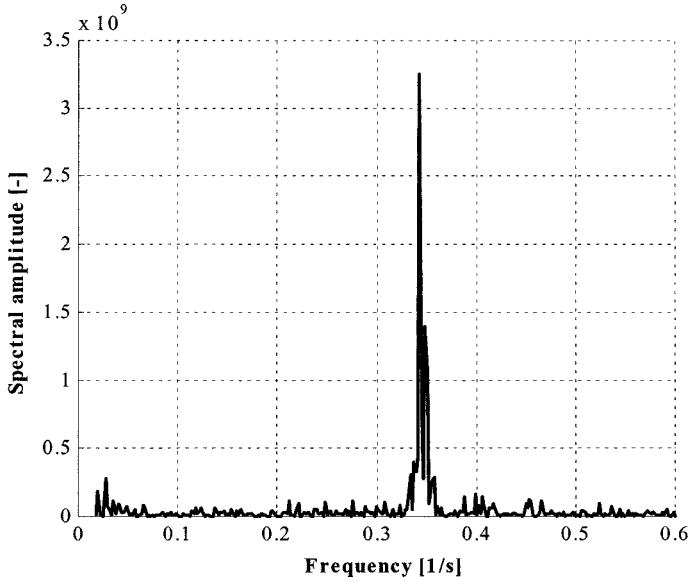

Fig. 4 Fourier spectrum of lift coefficient response from DVM at $U = 8$ m/s

attack. This was deemed to be interesting for validation purposes as the influence of the angle of attack on the aerodynamic forces is important in aeroelastic simulations involving rotation of bodies like the coupled two-degrees of freedom flutter phenomenon. The results for the mean lift coefficient in comparison to other investigations are shown in Fig. 5.

When a body moves in a fluid flow, it will be subjected to motion-dependent forces. These forces cause the so-called aerodynamic damping but they can also lead to instabilities of elastically mounted structures. A popular set of expressions for these forces is the one proposed for bridge deck analysis by Scanlan *et al.* (1971). It is based on the assumption that the self-excited lift and moment on a

Table 1 Results for Storeboelt Bridge aerodynamic simulations at zero angle of incidence

Source	$C_D = \frac{F_D}{\frac{1}{2}\rho U^2 D}$	$C_L = \frac{F_L}{\frac{1}{2}\rho U^2 B}$	$St = \frac{fD}{U}$
Morgenthal, McRobie, (DVM)	0.42	0.08	0.19
Jenssen and Kvelmsdal (1999), (FV)	0.45	0.04	0.16
Enevoldsen *et al.* (1999), (FV)	0.51	0.08	0.17
Larsen and Walther (1998), (DVM)	0.56	0.07	0.17
DMI and SINTEF (1993), (section model)	0.54	0.01	0.11-0.15
Larose (1992), (Taut strip model)	0.72	-0.08	0.11
Morgenthal (2000), (smoke tunnel)			0.19

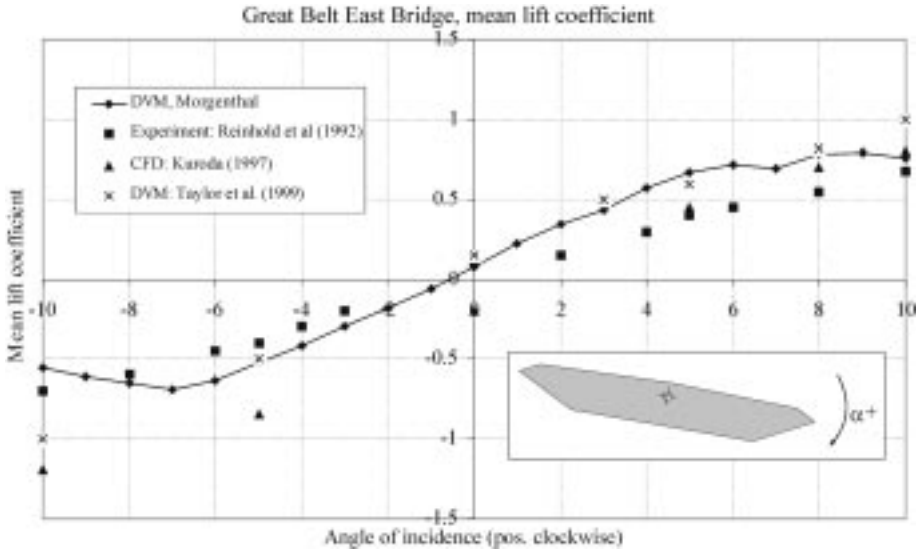

Fig. 5 Mean lift coefficient at various angles of incidence, DVM results for Storeboelt Bridge

bluff body may be treated as linear in the structural displacement and rotation and their first derivatives which reads in the complete formulation:

$$F_h(t) = \frac{1}{2}\rho U^2 B\left[KH_1^*(K)\frac{\dot{h}}{U} + KH_2^*(K)\frac{B\dot{\alpha}}{U} + K^2 H_3^*(K)\alpha + K^2 H_4^*(K)\frac{h}{B}\right]$$

$$F_\alpha(t) = \frac{1}{2}\rho U^2 B^2\left[KA_1^*(K)\frac{\dot{h}}{U} + KA_2^*(K)\frac{B\dot{\alpha}}{U} + K^2 A_3^*(K)\alpha + K^2 A_4^*(K)\frac{h}{B}\right] \quad (1)$$

where $h(t)$ and $\alpha(t)$ are the vertical and rotational section motion and $K = B\omega / U$ is the nondimensional ('reduced') frequency of motion of the bridge where B is the deck width. The nondimensional coefficients H_i^* and A_i^* are referred to as aerodynamic or flutter derivatives. As the derivatives are a function of the reduced frequency they can only be measured if the bridge is in a

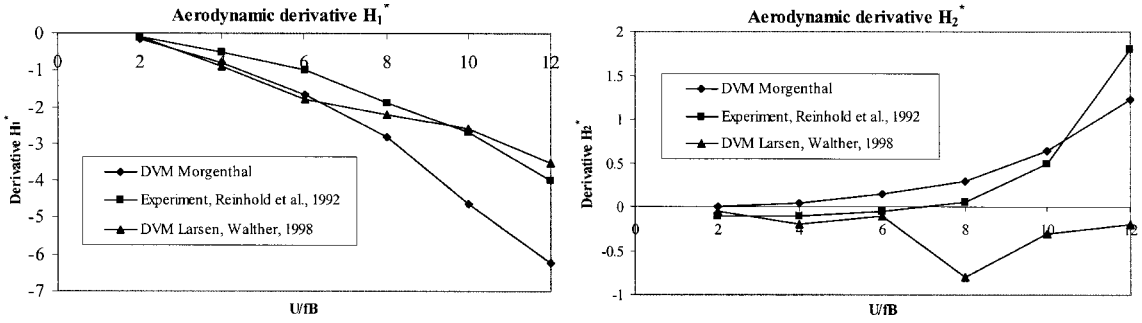

Fig. 6 Aerodynamic derivatives H_1^* and H_2^*

sinusoidal oscillatory state. Thus forced vibration tests are performed, the harmonic in the force signals is filtered out using a best-fit technique and the derivatives are calculated.

For the forced motion amplitudes of $0.04B$ and 3^o were used for vertical and rotational direction respectively. The aerodynamic derivatives H_1^* and H_2^* are shown for comparison in Fig. 6. Generally the agreement is reasonable as the shape of the graphs is captured.

2.2. Fluid-structure interaction analyses

A fluid-structure interaction routine in 2-D was implemented in the DVM code. For the 2D section analyses a structural system as shown in Fig. 7 was used. The coupling of the two degrees of freedom of the structural dynamics solution with the lift and moment forces of the fluid dynamics solution is done at every time step.

The Newmark-beta method in its unconditionally stable scheme of $\delta = 0.5$ and $\beta = 0.25$ was used to integrate the structural equations of motion forward in time. Structural damping was modelled as Rayleigh damping.

The FSI-routine implemented in the DVM was used to simulate vortex-induced vibrations. The Storebœlt Bridge used for calibration tests earlier also experienced those. Particularly the mode with five half-sine waves in the main span, having a natural frequency of 0.2 Hz, was prone to these oscillations. Therefore, the analyses focussed on simulating this structural mode. Interaction analyses were carried out at a range of wind speeds which cause vortex shedding frequencies close to the natural frequency of the vertical mode, to study the lock-in behaviour. Here the shedding process

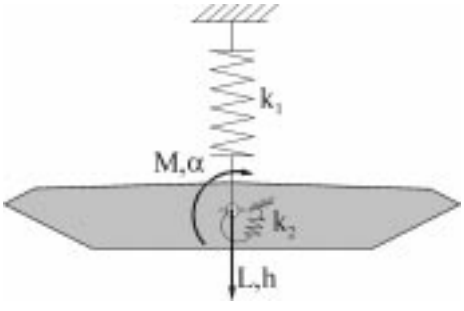

Fig. 7 Structural system considered

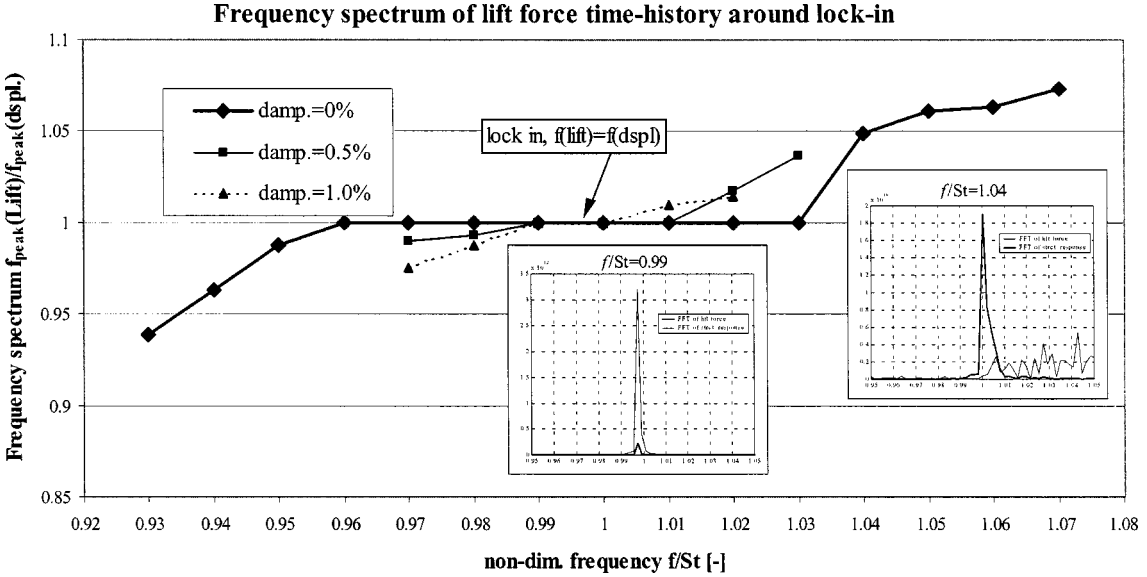

Fig. 8 Dominant shedding frequency with respect to the frequency of structural response around resonance point $f / St(D) = 1$ at various levels of structural damping

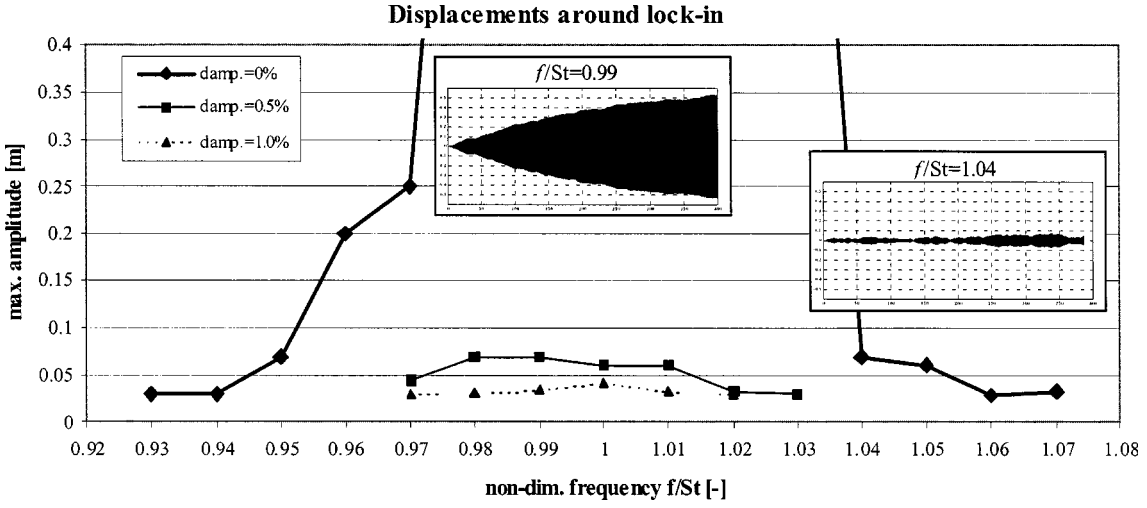

Fig. 9 Maximum amplitude observed around resonance point $f / St(D) = 1$ at various levels of structural damping

becomes controlled by the oscillatory motion of the bridge, and the shedding frequency remains locked in to this vibration. This leads to a widened range of resonance wind speeds, which is depicted in Fig. 8 where the results of a Fast Fourier Transformation of the time-histories of lift force and structural displacement are shown. At lock-in, these have a peak at the same frequency while off lock-in they drift away. In the diagram the lock-in region can be clearly seen. Analyses were performed for 3 levels of equivalent damping, namely 0%, 0.5% and 1.0% of critical and the diagrams clearly show a dependence of the width of the lock-in region on the damping. Structures

with high levels of damping have a significantly smaller lock-in region. As natural wind speeds fluctuate with time, these can thus be expected to show lower amplitudes. Maximum displacements observed in the simulations are plotted in Fig. 9. It has to be mentioned that for the undamped system unlimited amplitudes were observed at lock-in. This is contrary to common knowledge of vortex induced vibrations and may be due to the fact that the present numerical model does not take account of the randomness inherent in turbulent flow, which underlines the need to implement a diffusion model. However, further analyses will have to ascertain the reasons for this discrepancy.

2.3. Quasi-3D model

The DVM code has been extended such as to enable simulations of beam-type structures in a quasi three-dimensional manner. This is done by performing two-dimensional simulations of N sections parallel to one another. Initially these have the two-degree of freedom structural configuration introduced earlier. If the two-dimensional domains are now considered as slices of a beam, these can be coupled by forming a global stiffness matrix with $2N$ degrees of freedom thus considering the individual contributions from each slice to the three-dimensional response of the beam. This principle is depicted in Fig. 10.

It is important to note that for now coupling is only established by the structure – the interaction of the fluid-dynamic solutions has not been considered so far. This is a great simplification since the flow along the bridge is correlated and this interaction of the fluid solutions of the individual slices is neglected. However, for slices far enough apart this may not be very significant.

If a beam formulation with N slices is used, L_i, M_i and h_i, α_i are the corresponding nodal forces and displacements, respectively. These can be arranged in a stiffness matrix defined as follows:

$$\boldsymbol{K}\begin{bmatrix} h_1 \\ \dots \\ h_N \\ \alpha_1 \\ \dots \\ \alpha_N \end{bmatrix} = \begin{bmatrix} L_1 \\ \dots \\ L_N \\ M_1 \\ \dots \\ M_N \end{bmatrix} \tag{2}$$

the bending part of which was assembled using the standard 2-noded Hermitian beam element with

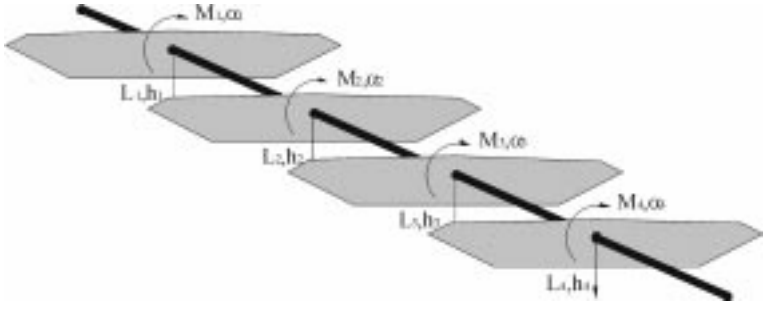

Fig. 10 Multi-section beam formulation

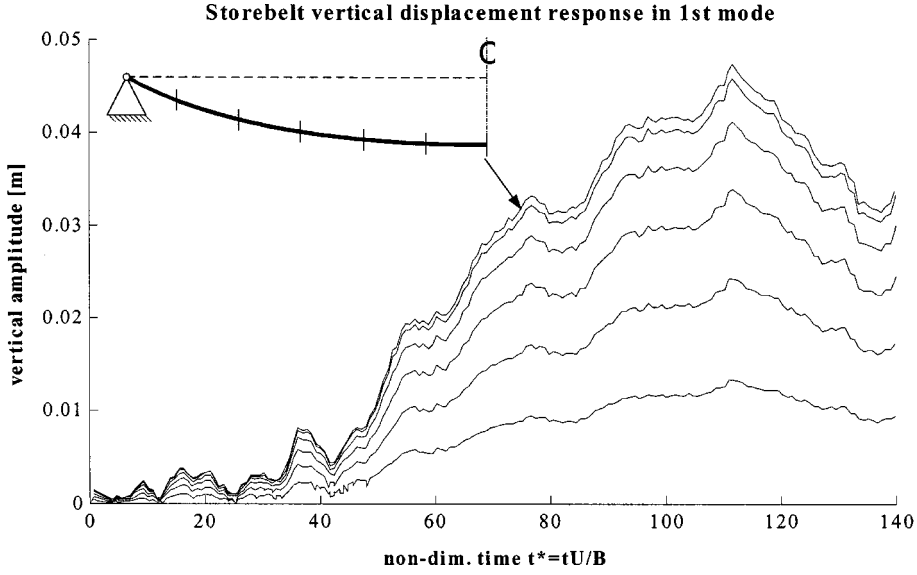

Fig. 11 Envelope of vibration at the different sections analysed using the quasi 3-D scheme

cubic polynomials as shape functions. The sub-matrices for bending and torsion remain decoupled. If the mass, damping (using Rayleigh damping) and stiffness matrices are assembled, the global system response can again be integrated forward in time.

Analyses on vortex induced vibrations of Storebœlt Bridge were repeated applying this method. The first vertical mode was studied, discretising the beam by 12 elements along its length and thus solving 11 DVM simulations simultaneously. Vortex induced oscillations could successfully be modelled. After an initial stage of uncorrelated fluid solutions all slices locked on to the oscillation of the bridge in the first mode and maximum amplitudes at mid-span were predicted as 5 cm. A diagram showing the growth in amplitude at the various sections is shown in Fig. 11. This simulation was done at zero damping and it is interesting to note, that the quasi 3-D method was able to predict the limited amplitude of the vortex-induced vibration.

3. The Finite Volume Method

3.1. Static bridge deck analyses

The Finite Volume code NEWT, developed by Dawes, Cambridge, is a fully 3-D compressible flow solver on tetrahedral unstructured meshes. It features moving meshes and solution-adaptive mesh refinement and has been used extensively in turbomachinery, e.g., Dawes 1993. The program was adopted for studies on vortex shedding and fluid-structure interaction problems in bridge aerodynamics, as will be described below.

The mesh used consists of approximately 50,000 cells, most of which were added to obtain a reasonable representation of the boundary layer at Reynolds numbers of the order of 10^7. Cells on the body surface were as small as 3 cm. The mesh is shown in Fig. 12. One layer of cells in depth was used, i.e., practically two-dimensional analysis performed. No turbulence model was employed at first, even though NEWT features both a standard k-ε model and Large Eddy Simulations.

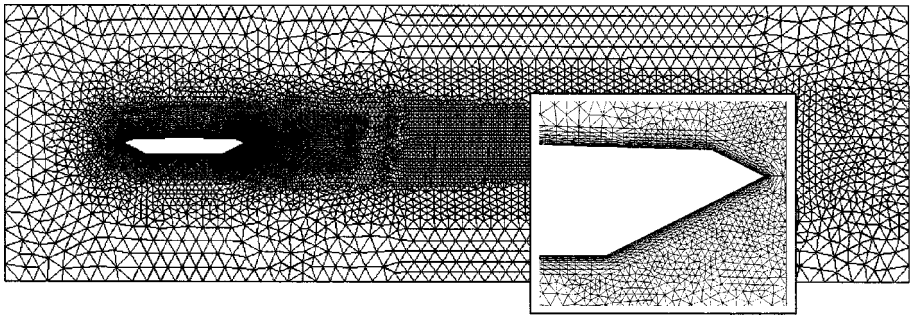

Fig. 12 Mesh used for FV calculations

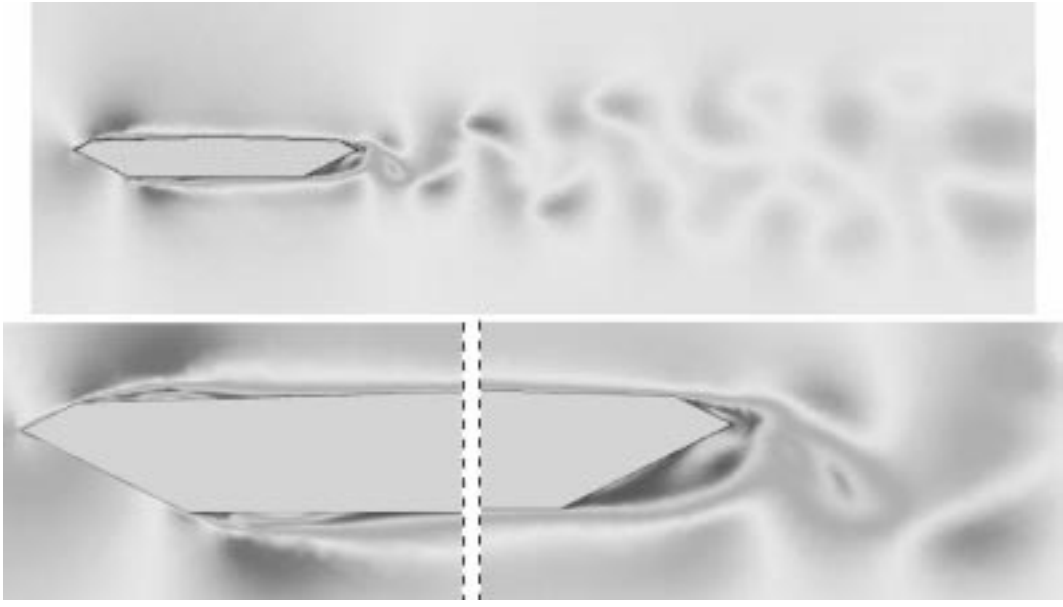

Fig. 13 Velocity contours, $U = 40$ m/s

Velocity contours of simulations at a flow velocity of 40 m/s are shown in Fig. 13.

3.2. Fluid-structure interaction analyses

The FV code NEWT was extended by a fluid-structure interaction routine, which basically operates in 2-D, as introduced for the DVM earlier.

It is obvious, that in order to simulate the oscillation of a solid embedded in a fluid flow the Finite Volume mesh has to be displaced according to the motion of the body surface boundaries. The position of the nodes on the surface is determined at each time step from the structural displacements, which were calculated by the structural dynamics solver. The surrounding mesh then needs to be adapted to the new surface position and there are various options for this. Here, the simplest method was applied, which is to linearly interpolate the displacements between the body surface and the fixed walls surrounding the domain. To this end, a meta-mesh of triangular elements

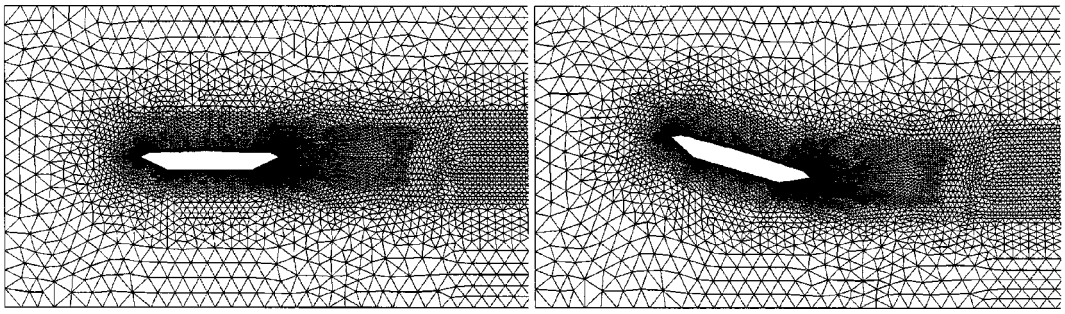

Fig. 14 Mesh adaption to body rotation, original (left) and modified mesh

was created covering the main mesh and having nodes on the body surface corners and walls. In these elements linear shape functions were employed to interpolate displacements. Each fluid mesh node is thus simply slaved to the bridge and the domain boundaries. An example showing the adaptation of the mesh to a rotation of the bridge deck is shown in Fig. 14.

The motion of the finite volumes through the mesh needs to be taken into account in the flux terms of the Finite Volume conservation equations. A procedure as outlined in Batina (1991) was adopted here. Coupling between the fluid and the structural dynamics is done by integrating the pressure distribution on the body at each time step and integrating the structural response forward in time, again using the Newmark-beta scheme.

Since the NEWT calculations are much more demanding than the DVM simulations in terms of computing power, only calculations as proof-of-concept could be performed so far. The Storebœlt cross-section was again used. The natural period was, however, altered such as to enable simulation of a reasonable number of cycles.

The simulation was started with an initial vertical displacement of the body h_0 corresponding to a static displacement under the average lift force. This was to study whether the fluid flow would cause the amplitudes to grow or to decay. This is a more efficient approach to flutter analysis than to start from rest and wait for the oscillations to build up. Fluid-structure interaction analyses were started from a swung-in fluid dynamics system as shown in Fig. 13. The at-rest position of the body then had to be associated with a displacement of h_0 as depicted in Fig. 15. Hence, the coordinate

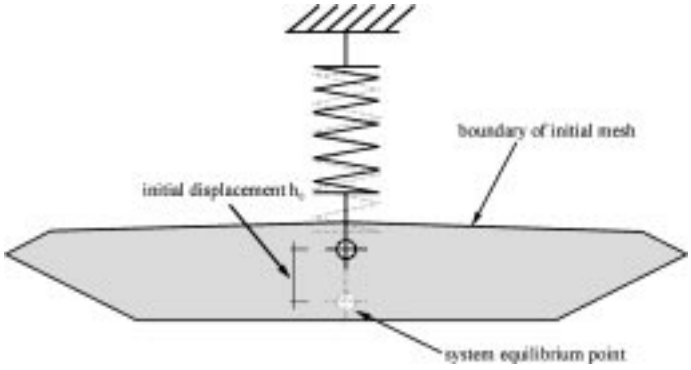

Fig. 15 Starting point of fluid-structure interaction analysis

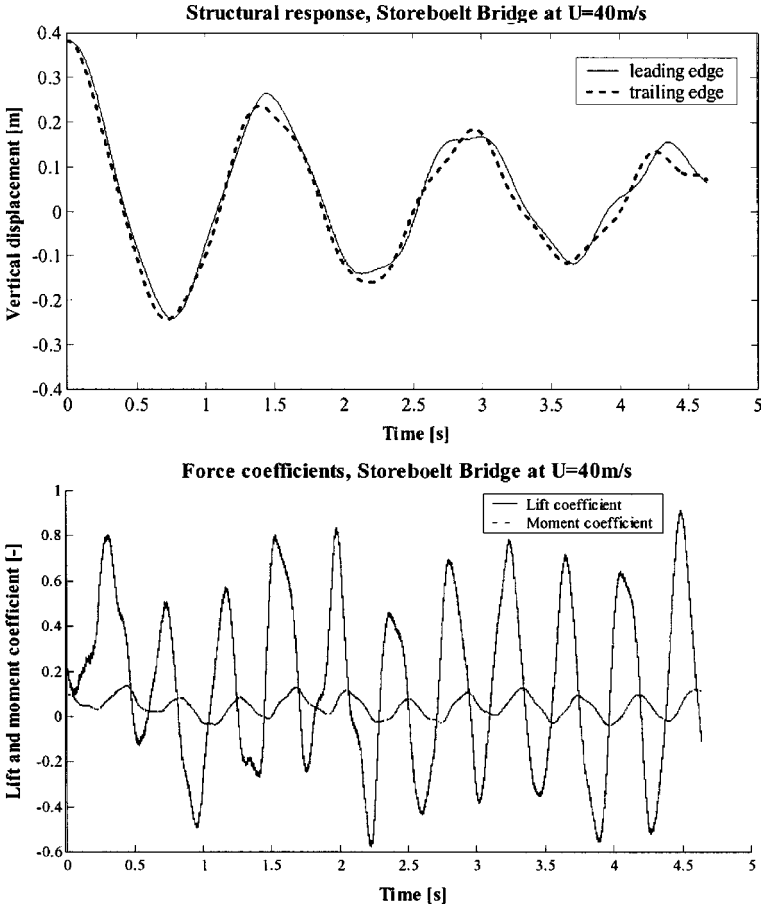

Fig. 16 Displacement response and aerodynamic forces, FSI-simulation on Storeboelt bridge deck

system for structural displacements was shifted by h_0.

The displacement response of the system and the fluid dynamic forces acting on the deck are shown in Fig. 16. The interaction between the motion of the deck and the forces is clearly visible. The amplitudes decay with time, which indicates that the system is stable under the given conditions. However, it would clearly be necessary to run the simulation for more cycles of structural response to draw conclusions from it. As a proof-of-concept the simulations were, however, successful and the implementation of the fluid structure interaction module into the new parallel computing version of NEWT will enable more thorough calculations in the future.

4. Conclusions

Discrete Vortex and Finite Volume formulations have been investigated to shed light on the question as to which numerical method is best suited for the various aerodynamic applications in long-span bridge design. Generally both methods are applicable as they are capable of modelling the complex phenomena involved in the process of vortex shedding from bluff bodies.

The DVM is particularly well suited to bluff body aerodynamics as discretisation of vorticity with

a grid-free scheme is done only in regions where circulation is actually present. This reduces the computational cost whilst still modelling the small-scale vortical structures inherent in the flow. The grid-free nature also eases the analysis of bodies with complicated geometries. In particular, the DVM is well suited to the analysis of problems with moving body surfaces. It has, however, to be highlighted that the calibration process of the DVM is more difficult and subtle than for other methods. The numerical procedure involving factors like surface vorticity release, convection and diffusion, vortex merging and their interaction makes it more difficult to obtain clear signals.

Analyses using the FV method clearly show that more effort has to be put into pre- and post-processing. Capturing the small-scale structures and modelling such complex phenomena like separation and reattachment requires a mesh suitably refined at important regions. Here, solution adaptive mesh refinement can prove favourable both in terms of arriving at an appropriate mesh density throughout the domain and in terms of computational cost.

Application in a design environment could see the Discrete Vortex Method in favour. It is easy to apply as no grid is used and thus results can be achieved fairly quickly. Changes in body shape, however, require re-calibration of numerical parameters. Here, the FVM is more versatile and thus more readily usable.

Calculations of three-dimensional fluid-structure interaction still seem not to be feasible with the computing power available. In long-span bridge design this is not a major drawback as higher mode contributions are generally low and thus a 2-D section model can well represent the structural behaviour. Furthermore, analytical modal decomposition methods exist and the input parameters in the form of aerodynamic derivatives can be obtained from 2-D methods. Furthermore, pseudo-3D methods as discussed herein present a scope for further work.

References

Batina, J.T. (1991), “Dynamic mesh for complex-aircraft aerodynamic analysis”, *AIAA J.*, **29**, 328-331.

Dawes, W.N. (1993), “Simulating unsteady turbomachinery flows on unstructured meshes which adapt both in time and space”, *Proc. of the '93 Int. Gas Turbine and Aeroengine Congress and Exposition Cincinnati*, Ohio.

Deniz, S. and Staubli, T. (1998), “Oscillating rectangular and octagonal profiles: modelling of fluid forces”, *J. Fluid. Struct.*, **12**, 859-882.

DMI and SINTEF (1993), “Wind-tunnel tests, Storebœlt East Bridge, Tender evaluation, suspension bridge, alternative sections, section model tests”, Technical Report 91023-10.00, Rev. 0, Danish Maritime Institute, Lyngby, Denmark.

Enevoldsen, I., Hansen, S.O., Kvamsdal, T., Pedersen, C. and Thorbek, L.T. (1999), “Compuatational wind simulations for cable-supported bridges”, *Proc. the 10th Int. Conf. Wind Eng.* '99, Copenhagen.

Frandsen, J.B. and McRobie, F.A. (1999), “Computational aeroelastic modelling to guide long-span bridge cross-section design”, *Proc. the 10th Int. Conf. Wind Eng.* '99, Copenhagen.

Jenssen, C.B. and Kvelmsdal, T. (1999), “Computational methods for fsi-simulations of slender bridges on high performance computers”, in: *Computational Methods for Fluid-Structure Interaction*, T. Kvalmsdal *et al*. (editor), Tapir.

Kuroda, S. (1997), “Numerical aspects of the final design of the 1624 m suspension bridge across the great belt”, *J. Wind Eng. Ind. Aerod.*, **67-68**, 239-252.

Larose, G.L. (1992), “The response of a suspension bridge deck to turbulent wind: the taut strip model approach”, M.Eng.Sc. Thesis, The University of Western Ontario, Ontario.

Larsen, A. and Walther, J.H. (1998), “Discrete vortex simulation of flow around five generic bridge deck sections”, *J. Wind Eng. Ind. Aerod.*, **77-78**, 591-602.

Leonard, A. (1980), “Vortex methods for flow simulation”, *J. Comp. Phys.*, **37**, 289-335.

Morgenthal, G. (2000), “Comparison of numerical methods for bridge-deck aerodynamics”, MPhil Thesis,

University of Cambridge.
Reinhold, T.A., Brinch, M. and Damsgaard, A. (1992), "Wind tunnel tests for the great belt link", Aerodynamics of Large Bridges (editor Larsen, A.), *Proc. the 1st Int. Symp.*, 1992, Copenhagen, Denmark.
Scanlan, R.H. and Tomko, J.J. (1971), "Airfoil and bridge deck flutter derivatives", *J. Eng. Mech.*, ASCE, **97**, 1717-1737.
Taylor, I.J. and Vezza, M. (1999), "Analysis of the wind loading on bridge deck sections using a discrete vortex method", *Proc. the 10th Int. Conf. on Wind Eng. '99*, Copenhagen.